



Long Non-Coding RNA CCAT2 Activates RAB14 and Acts as an Oncogene in Colorectal Cancer

Dalu Wang, Zhilong Li and Hongzhan Yin*

Department of General Surgery, Shengjing Hospital of China Medical University, Shenyang, China

OPEN ACCESS

Edited by:

Hanqing Liu,
Jiangsu University, China

Reviewed by:

Wei Cao,
Shanghai Jiao Tong University, China
Minggang Fang,
University of Massachusetts Medical
School, United States

*Correspondence:

Hongzhan Yin
yinhz@sj-hospital.org

Specialty section:

This article was submitted to
Cancer Molecular Targets
and Therapeutics,
a section of the journal
Frontiers in Oncology

Received: 02 August 2021

Accepted: 07 October 2021

Published: 19 November 2021

Citation:

Wang D, Li Z and Yin H (2021)
Long Non-Coding RNA CCAT2
Activates RAB14 and Acts as an
Oncogene in Colorectal Cancer.
Front. Oncol. 11:751903.
doi: 10.3389/fonc.2021.751903

Here, we investigated the clinicopathological and prognostic potential of the long noncoding RNA Colon Cancer-Associated Transcript 2 (CCAT2) in human colorectal cancer (CRC). We used qPCR to quantify CCAT2 levels in 44 pairs of CRC tissues and adjacent nontumor and healthy colon mucosa tissues, and in several CRC cell lines (SW620, SW480, HT-29, LOVO, HCT116 and DLD-1) and normal human colorectal epithelial cells (HFC). We assessed the effects of CCAT2 overexpression or knockdown on the proliferation, migration and invasion by SW620 and LOVO cells using CCK-8, transwell, and wound-healing assays, respectively. We also investigated the potential interaction between CCAT2 and TAF15 through RNA pull down and rescue experiments. Lastly, we evaluated the expression of the cell cycle progression markers and GSK3 β signaling pathway proteins using Western blotting. Our results showed that CCAT2 was upregulated in CRC tissues and cell lines as compared to controls. Ectopic expression of CCAT2 promoted CRC cell proliferation, migration and invasion, likely through direct interaction with TAF15, transcriptional activation of RAB14, and activation of the AKT/GSK3 β signaling pathway. *In vivo*, CCAT2 promoted CRC cell growth and metastasis in nude mice. Taken together, these results highlight the actions of CCAT2 as a CRC oncogene.

Keywords: LncRNA, CCAT2, colorectal cancer, TAF15, RAB14

INTRODUCTION

Colorectal cancer (CRC) is the third most common malignancy worldwide affecting more than 1.2 million people every year and is the fourth leading cause of cancer-associated mortality, causing more than 600,000 yearly deaths (1). CRC incidence is higher among men than among women and strongly increases with age (2). CRC has both hereditary and environmental causes that contribute to the gradual development of the disease through the adenoma-carcinoma sequence. CRC therapies include surgery, adjuvant radiotherapy, adjuvant chemotherapy, fluorouracil-based chemotherapy, and oxaliplatin adjuvant treatment, among others, which are applied depending on the pathological stage of each patient (3, 4). Some patients develop radioresistance resulting in poor prognosis, which could be alleviated by early detection (5).

Abbreviations: CRC, Colorectal cancer; lncRNAs, long noncoding RNAs; CCAT2, colon cancer-associated transcript 2; IF, immunofluorescence; EMT, epithelial-mesenchymal transition; RIP, RNA immunoprecipitation.

Recently, non-coding RNAs have been proposed as potential diagnostic and prognostic biomarkers for several types of cancer (6, 7). Long non-coding RNAs (lncRNAs) can function as decoy, scaffold, guide, and enhancer RNAs, and participate as short nucleic acid strands in chromatin remodeling, transcriptional and post-transcriptional regulation, and epigenetics (8–10). Several lncRNAs have been linked to various types of cancer; for example, terminal differentiation-induced non-coding RNA (TINCR), lncRNA-p21, lncRNA OIP5-AS1, lncRNA UCA1 and Hox transcript antisense intergenic RNA (HOTAIR) have been identified as potential therapeutic targets for cancer treatment (11, 12). In addition, lncRNA such as RC3H2, TANRIC, PTENP1 FOXD2-AS1 has been identified as diagnostic or prognostic predictor for various types of cancer (13–16).

lncRNA colon cancer-associated transcript-2 (CCAT2) expression is cell- and tissue-specific and localizes mainly to the nucleus of cells. CCAT2 is a 1752-base RNA transcribed from the 8q24 region of the human genome containing a single nucleotide polymorphism (SNP), rs6983267. The rs6983267 SNP has been associated with an increased risk of colorectal, prostate, ovarian and breast cancers (17–19). The genomic region spanning rs6983267 contains DNA enhancer elements that bind to transcription factor 7-like 2 (TCF7L2) and β -Catenin, and induce the production of cancer stem cell (CSCs). Overexpression of CCAT2 has been linked to various types of cancer, including CRC, breast, lung, esophageal squamous cell carcinoma, and gastric cancers. Indeed, this lncRNA promotes

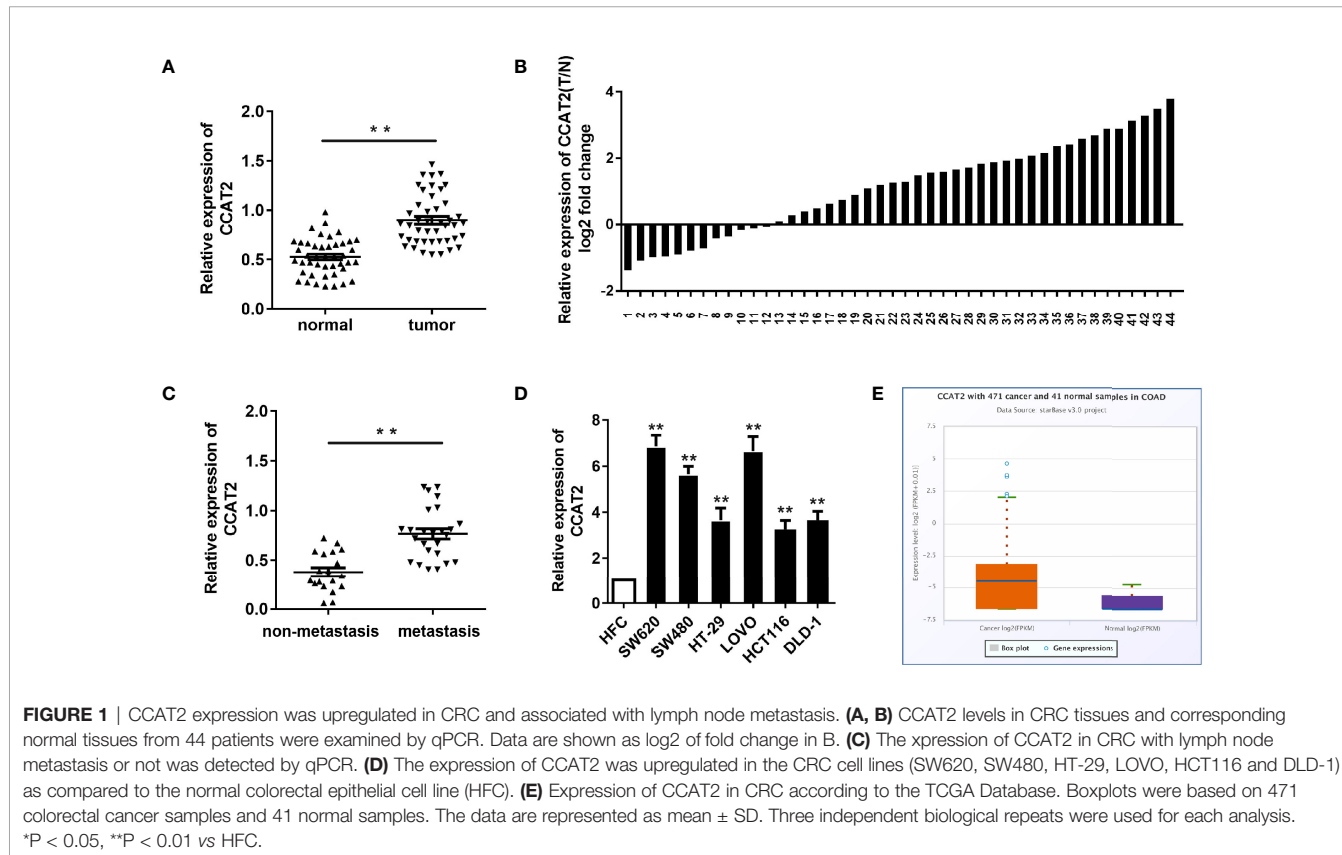
tumor growth and metastasis while causing reduced sensitivity to chemotherapy (20–26).

In this study, we investigated lncRNA CCAT2 expression in CRC tissues and cell lines. *In vitro*, CCAT2 overexpression promoted cell proliferation, migration and invasion by activating the RAB14 transcription factor and the AKT/GSK3 β signaling pathway in CRC tissues and cell lines. Our results suggest that elements in the CCAT2/RAB14/AKT/GSK3 β axis may serve as potential prognostic and diagnostic biomarkers to treat CRC.

RESULTS

CCAT2 Expression Was Upregulated in CRC and Correlated With Lymph Node Metastasis

In order to assess CCAT2 expression, we first examined the levels of CCAT2 in 44 paired colorectal cancer (CRC) and adjacent normal tissues *via* qPCR. Our results revealed that CCAT2 was upregulated in CRC tissues (Figures 1A, B). Furthermore, we measured CCAT2 levels in CRC with and without lymph node metastasis and found that CCAT2 was upregulated in the former case but not the latter (Figure 1C). In addition, qPCR also showed upregulation of CCAT2 in a CRC cell line (Figure 1D). The Cancer Genome Atlas (TCGA) database also indicated elevated CCAT2 expression in CRC (Figure 1E). Together,



these results demonstrated that CCAT2 was upregulated in CRC and promoted metastasis, suggesting that CCAT2 might act as an oncogene in CRC.

Ectopic Expression of CCAT2 Promoted Cell Proliferation in CRC

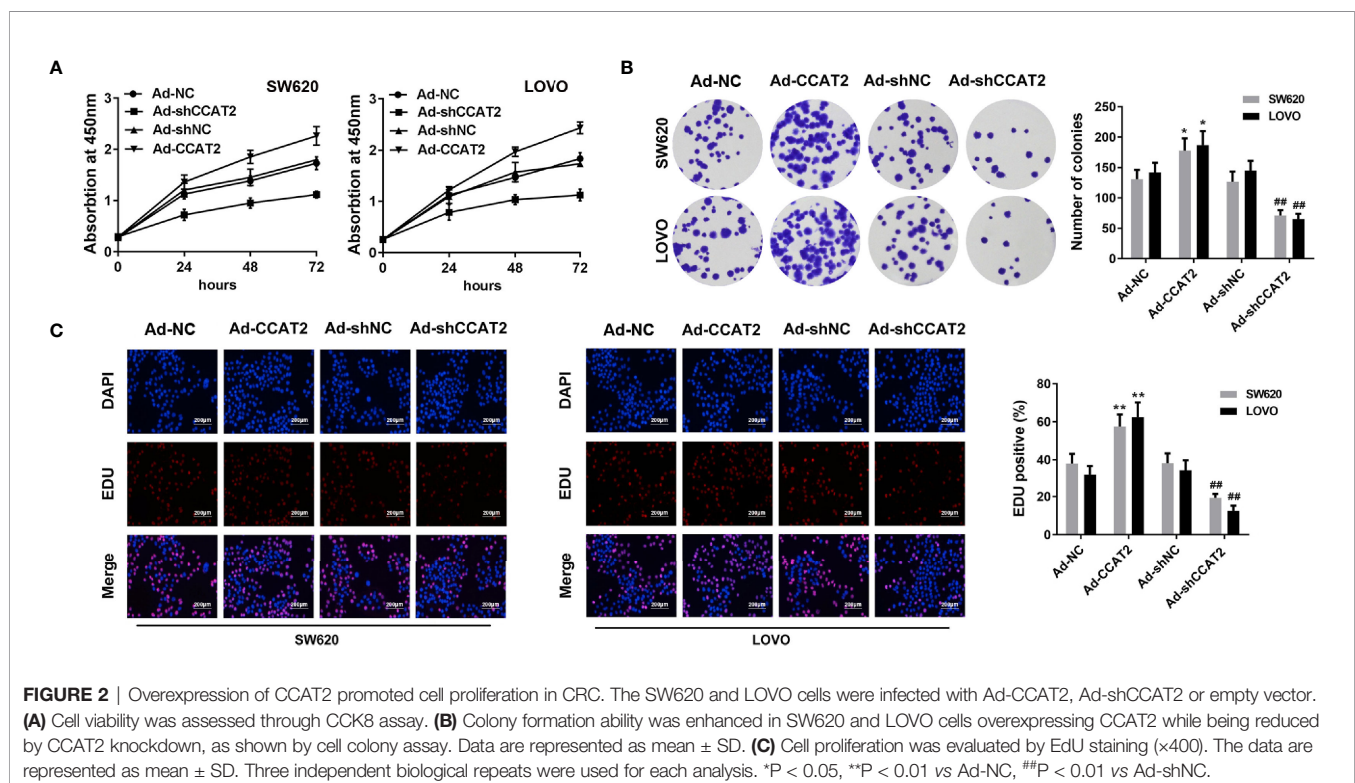
CCK8 and colony-forming assay showed that the ectopic expression of CCAT2 enhanced the proliferation and colony formation of SW620 and LOVO cells (Figures 2A, B). However, the knockdown of CCAT2 had the reverse effects. In addition, we performed EdU staining to further validate these findings. Expectedly, our results showed a higher presence of EdU-positive cells among those with elevated expression of CCAT2, and knockdown of CCAT2 dramatically reduced the number of EdU-positive cells (Figure 2C). Thus, these results indicated that CCAT2 promoted colorectal cancer cell proliferation *in vitro*.

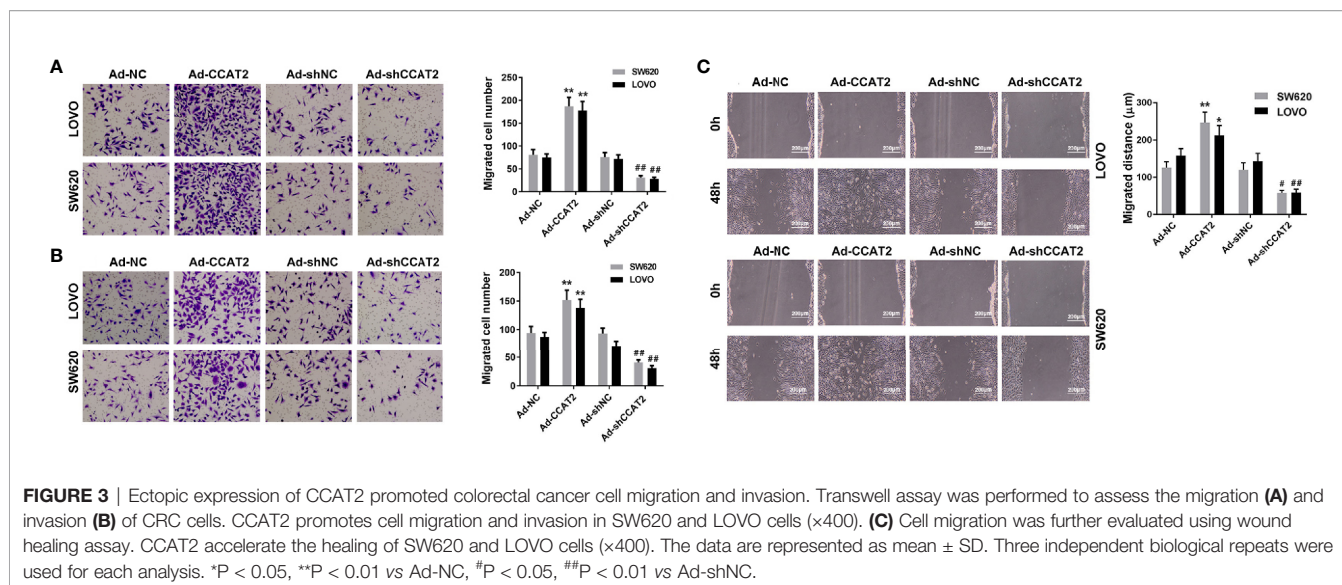
Ectopic Expression of CCAT2 Promoted Colorectal Cancer Cell Invasion, Migration and Wound-Healing

To study whether CCAT2 is involved in colorectal cancer metastasis, we evaluated the effects of CCAT2 on the migration and invasion of colorectal cancer cells. Overexpression of CCAT2 promoted the migration and invasion of SW620 and LOVO cells (Figures 3A, B). Wound-healing assay revealed that colorectal cancer cells infected with Ad-CCAT2 migrated faster than those infected with Ad-NC while cells infected with Ad-sh-CCAT2 migrated more slowly than those infected with Ad-shNC (Figure 3C). The overexpression of CCAT2 promoted colorectal cancer cell invasion, migration and wound-healing.

CCAT2 Promoted RAB14 Transcription Through Interaction With TAF15

To elucidate the molecular mechanism underlying the effects of CCAT2 on CRC cells, we performed RNA pull down and mass spectrometry analyses. We found that CCAT2 might directly bind with TAF15 (Figures 4A, B). Then, RIP assay was performed to further assess whether TAF15 could bind CCAT2 (Figure 4C). Furthermore, catRAPID software (http://s.tartagliab.com/page/largeRNAs_group) was used to predict the potential interaction between CCAT2 and TAF15. Our results indicated a high probability of interaction between them (Figure 4D). We then performed nuclear and cytoplasmic isolation of SW620 and LOVO cells, and qPCR analysis revealed that CCAT2 was mainly located in the nucleus (Figure 4E), in agreement with the results of FISH experiments (Figure 4F). Therefore, we focused our study on the transcriptional regulation of CCAT2 and TAF15. Starbase software (<http://starbase.sysu.edu.cn/index.php>) highlighted RAB14 as a potential gene target of TAF15. To test whether TAF15 might transcriptionally activate RAB14, we used a luciferase reporter assay in SW620 and LOVO cells. Our results showed that enforced expression of CCAT2 and TAF15 dramatically increased the luciferase activity of the reporter vector containing the promoter region of RAB14 while knockdown of CCAT2 or TAF15 reduced that activity (Figures 4G, H). We then performed ChIP assay and the results indicated that CCAT2 overexpression promoted the binding between TAF15 and promoter of RAB14. On the contrast, CCAT2 silencing inhibited that (Figure 4I). Afterwards, SW620 cells were transfected with CRISPR-Cas9





to knock out TAF15 and total RNA extraction showed that the mRNA expressions of TAF15 and RAB14 were downregulated compared to those in wild type cells (Figure 4J). Furthermore, our results from Western blots showed that overexpression of CCAT2 or TAF15 increased the protein levels of RAB14 while knockdown of CCAT2 or TAF15 reduce the protein levels of RAB14 (Figures 4K, L). Taken together, these results suggest that CCAT2 interacts with TAF15 and promotes the expression of RAB14.

Reduced Expression of RAB14 Inhibits the Proliferation-Enhancing Effect of CCAT2 on CRC Cells *In Vitro*

We transfected Ad-CCAT2-infected SW620 and LOVO cells with si-RAB14 to investigate effects of RAB14 on CCAT2 in CRC cells. After transfection, CCK8, colony formation, and EdU staining assays were employed to examine the proliferation of SW620 and LOVO cells. CCAT2 increased the proliferation of SW620 and LOVO cells, an effect that was reduced after transfection with si-RAB14, as strikingly apparent 72 h post-transfection (Figure 5A). Moreover, the colony (Figure 5B) and EdU-positive cell (Figure 5C) number were decreased after si-RAB14 transfection (Figures 5B, C). Taken together, our results suggested that RAB14 knockdown inhibited the proliferative effect of CCAT2 on CRC cells.

RAB14 Knockdown Inhibits the Migration- and Invasion-Enhancing Effects of CCAT2 on CRC Cells

We further investigated the effects of CCAT2 on the migration and invasion of Ad-CCAT2-infected SW620 and LOVO cells transfected with si-RAB14. Our results showed that RAB14 knockdown inhibited the migration and invasion-enhancing effects of CCAT2 on CRC cells (Figures 6A, B). Furthermore, results from our wound-healing assays indicated that CRC cells co-transfected with si-RAB14 and Ad-CCAT2 displayed a

reduced healing ability compared with those transfected with Ad-CCAT2 alone (Figure 6C).

CCAT2 Activated the AKT/GSK3 β Signaling Network, and Promoted Cell Cycle Progression and EMT via RAB14

To better understand the mechanistic link among the factors underlying the regulation of CCAT2 in CRC, we tested whether the upregulation of CCAT2 affected the AKT/GSK3 β signaling pathway. Our results indicated that CCAT2 overexpression enhanced AKT and GSK3 β activity in SW620 and LOVO cells. We also measured the levels of Cyclin D1, Cyclin E1 and p21, which contribute to cell cycle progression and are important components of the Wnt/ β -catenin signaling pathway. We found that CCAT2 activated the Wnt/ β -catenin signaling pathway through activation of nuclear β -catenin. To further understand the underlying mechanism by which CCAT2 induced migration and invasion of SW620 and LOVO cells, we evaluated the expression of EMT-related proteins. CCAT2 upregulated the expression of Vimentin, and N-cadherin (Figures 7A, B). Moreover, these effects were rescued by RAB14. In brief, all these data indicated that CCAT2 might promote proliferation, migration and invasion by activating the RAB14/AKT/GSK3 β signaling pathway in CRC cells.

CCAT2 Promotes CRC Cell Growth and Metastasis in Nude Mice

To further assess the biological roles of CCAT2 in tumorigenesis, we constructed a xenograft nude mouse model (Figure 8A). SW620 cells infected with Ad-CCAT2, Ad-shCCAT2 or their controls were subcutaneously injected into the back of nude mice, and tumor volume and weight were measured. CCAT2 promoted the growth of SW620 cells while CCAT2 knockdown inhibited it (Figures 8B, C). Bioluminescent imaging was used to detect SW620 metastasis. Remarkably, the metastasis of luciferase-tracking SW620 cells was promoted by CCAT2 overexpression but inhibited by CCAT2 knockdown (Figure 8D). Furthermore,

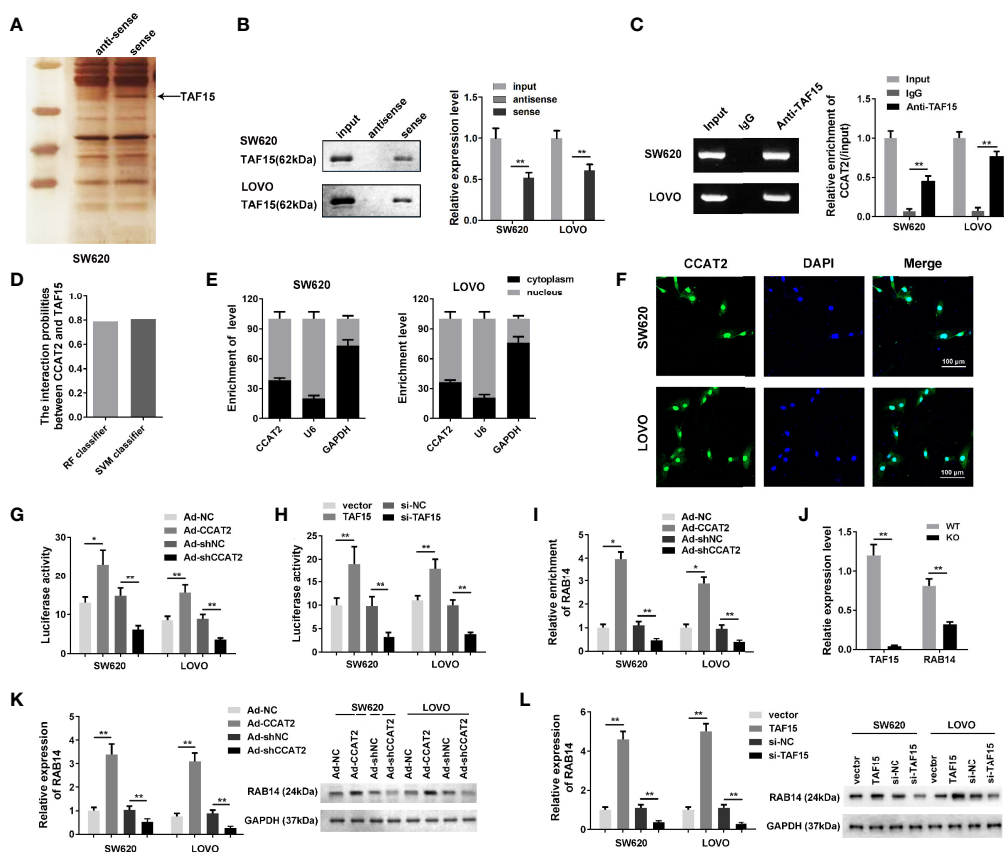


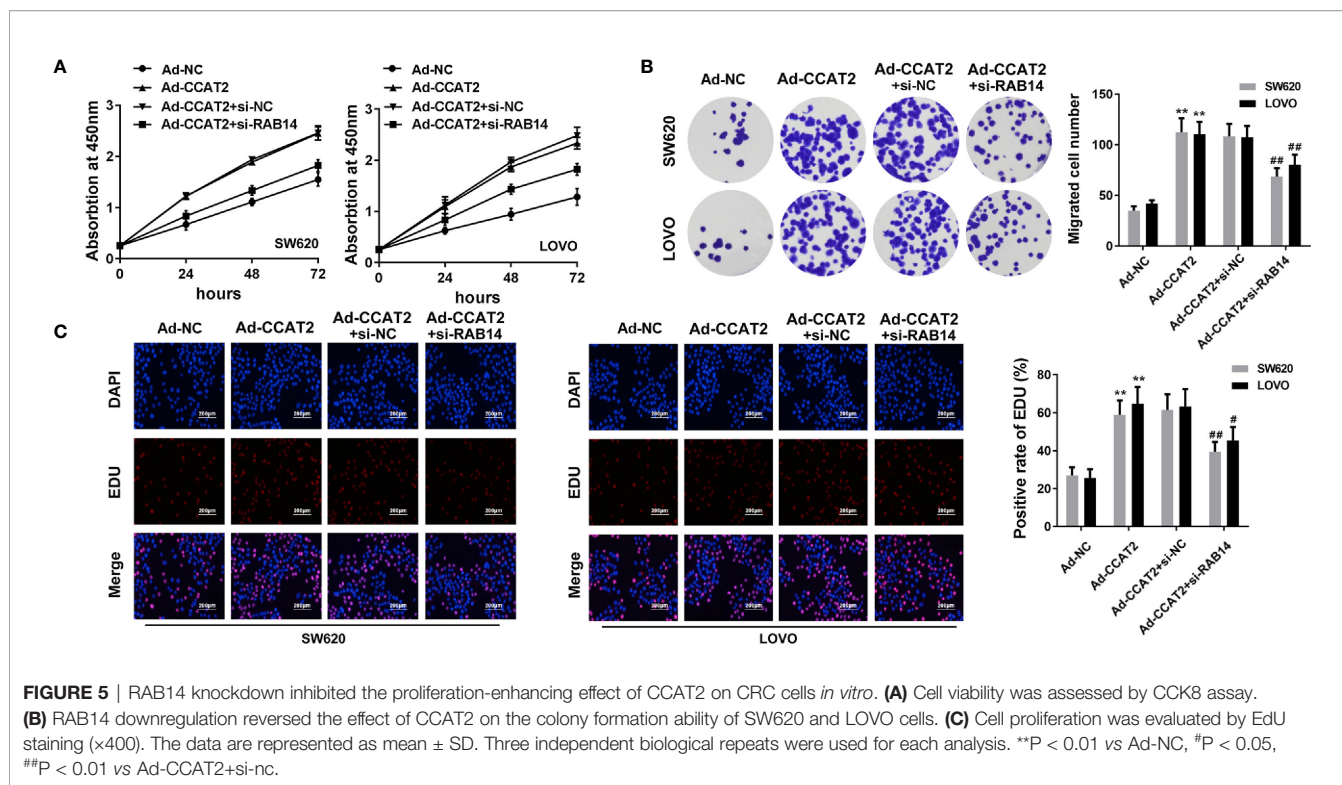
FIGURE 4 | CCAT2 regulated the expression level of RAB14 *via* interaction with TAF15. **(A, B)** The RNA pull down assay was carried out by biotinylated CCAT2 probe and silver staining to reveal the factors underlying the mechanism of CCAT2 in CRC cells. Mass spectrometry analysis highlighted TAF15 as a potential factor interacting with CCAT2 **(A)**. The interaction of CCAT2 and TAF15 was further verified by Western blot **(B)** and RIP assay **(C)**. **(D)** Bioinformatic prediction showing the potential interaction of CCAT2 and TAF15. **(E)** The cellular localization of CCAT2 as determined through nuclear and cytoplasmic separation test and qPCR. **(F)** FISH was performed to determine the localization of CCAT2 in the cells. **(G, H)** The transcriptional activity of RAB14 was measured by dual luciferase reporter assay in SW620 and LOVO cells after being infected or transfected with Ad-CCAT2, Ad-shCCAT2, TAF15, si-TAF15 and their corresponding controls. **(I)** ChIP analysis indicated that CCAT2 promoted the binding between TAF15 and the promoter of RAB14 while CCAT2 knockdown inhibited that. **(J)** Measurement of TAF15 and RAB14 levels by qPCR. Total RNA was extracted from SW620 cells that were transfected with CRISPR/Cas9 to knockdown TAF15. **(K, L)** Expression of RAB14 in cells infected with Ad-CCAT2, Ad-shCCAT2, TAF15, or si-TAF15 as measured by Western blot. Protein levels are shown as bar graphs. The data are represented as mean \pm SD. Three independent biological repeats were used for each analysis. * $P < 0.05$, ** $P < 0.01$.

HE staining revealed that the overexpression of CCAT2 altered the phenotypes of SW620 cells while CCAT2 knockdown inhibited such alterations (**Figure 8E**). IHC results indicated that CCAT2 promotes the expression of p-AKT, p-GSK3 α , cyclin D1 and cyclin E1 while knockdown of CCAT2 inhibited that (**Figure 8F**). These results suggested that CCAT2 promoted the growth and metastasis of CRC cells *in vivo*.

DISCUSSION

Colorectal cancer (CRC) is the third most common cancer malignancy worldwide. The dysregulation of lncRNAs can promote cell proliferation, resistance to apoptosis, angiogenesis, metastasis, and evasion of tumor suppressors,

and is associated with several pathophysiological processes, including cancer, neurodegeneration, as well as autoimmune and cardiovascular diseases (27, 28). The lncRNA CCAT2 is oncogenic in colon cancer and CCAT2 gene polymorphisms are linked to several types of cancer such as colon, kidney, thyroid, larynx, lung and myeloid cancers in different populations (29–32). CCAT2 has been used as a diagnostic and prognostic biomarker in the treatment of colorectal cancer. In this study, we validated the upregulation of CCAT2 in CRC tissues. Overexpression of CCAT2 remarkably enhanced the proliferation, invasion and wound healing potential of the SW620 and LOVO cells. Previously, *in vivo* research investigated the effect of CCAT2 overexpression in HCT116 cells. Here, we assessed the effects of both overexpression and knockdown of CCAT2 on the growth of SW620 cells. Our results

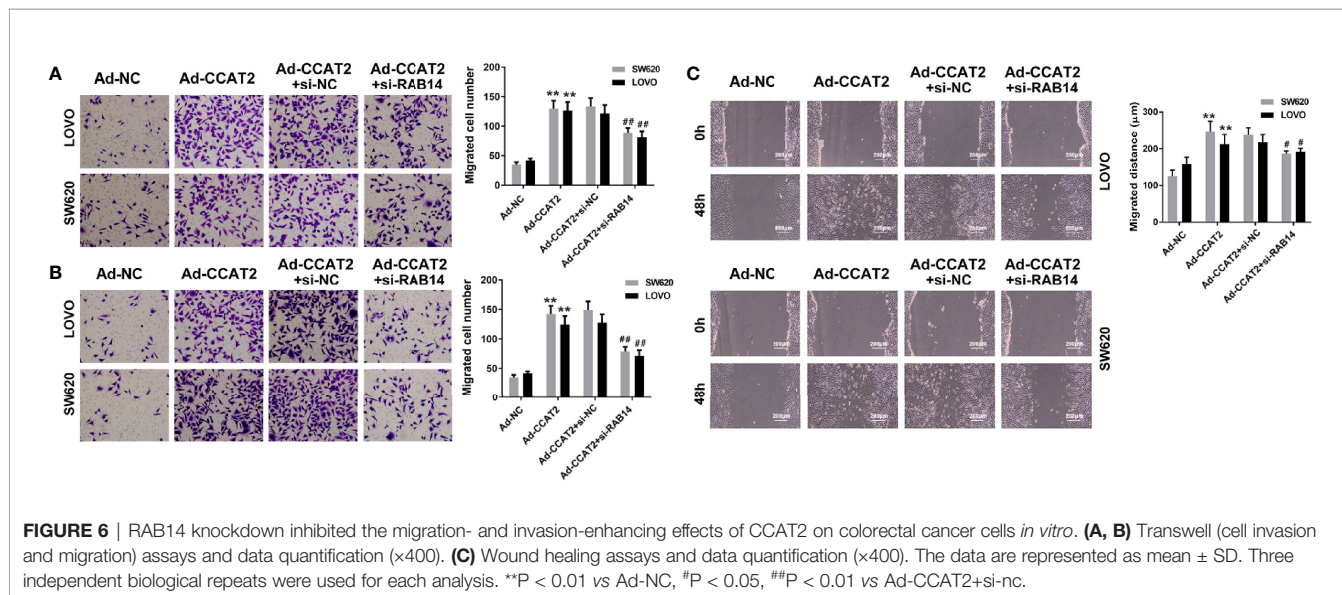


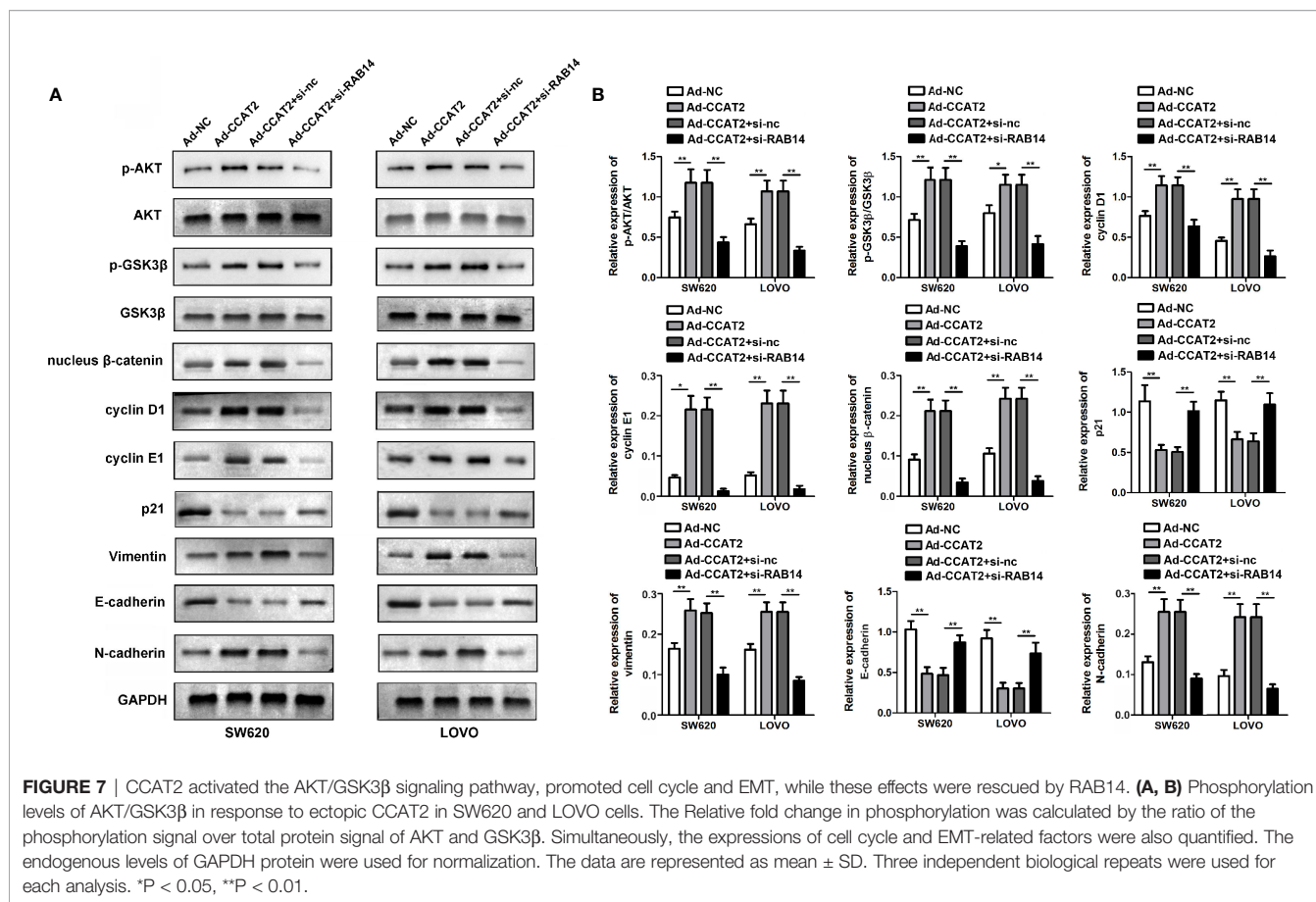
confirmed that CCAT2 promoted the metastasis of SW620 cells *in vivo*, thereby suggesting that it acts as an oncogene in CRC.

To further explore the underlying mechanisms by which CCAT2 acts as an oncogene in CRC, we evaluated its subcellular localization and found that CCAT2 was located mainly in the nucleus. Thus, we hypothesized that CCAT2 may be involved in epigenetic regulation. To test this hypothesis, we performed RNA pull down and mass spectrometry analyses. Our results suggested that CCAT2 might directly bind with TAF15. LncRNA Transient receptor

potential cation channel subfamily M member 2-AS (TRMP-AS), an antisense transcript of the *TRMP2* gene, promotes the proliferation of CRC cells by directly enhancing the activity of RNA-binding protein (RBP) TAF 15, which stabilizes *TRMP2* mRNA (33). Using starBase software, we identified TAF15 target genes and found that TAF15 and CCAT2 directly promote the transcriptional activity of *RAB14*.

The majority of Rab proteins promote cancer progression. Rab14 is a member of the RAS oncogene family of small GTPase proteins (34). Rab proteins participate in phagosomal systems and





biosynthetic/recycling pathways such as vesicle trafficking, signal transduction and receptor recycling (35). MicroRNA-451 (miR-451) and miR-338-3p act as tumor suppressors in human non-small-cell lung carcinoma (NSCLC) by targeting Ras-related protein 14 (36). Choroideremia-like protein (CHML), a member of the Rab escort protein (REP) family, promotes migration, invasion and metastasis of hepatocellular carcinomas (HCC) cells by facilitating Rab14 recycling (37). GSK3 β , a member of the GSK3 family of serine/threonine protein kinases, is aberrantly activated in various cancer types, including colorectal cancer (38–41). Tumor necrosis factor alpha (TNF α), a pro-inflammatory cytokine, induces epithelial-mesenchymal transition (EMT) in human HCT116 cells and thereby promotes CRC invasion and metastasis (37). EMT is a hallmark of the initiation and early growth of primary epithelial cancers (42–45); it gives cells the ability to metastasize and invade tissues, confers them stem cell characteristics, reduces apoptosis and aging, and promotes immunosuppression. However, the mechanistic link between RAB14 and the AKT/GSK-3 β signaling remains obscure (46). Here, we found that CCAT2 promoted the growth and metastasis of CRC cells by targeting TAF15 to enhance the transcriptional activation of RAB14, followed by the activation of the AKT/GSK3 β signaling pathway.

Our findings elucidated the underlying mechanism by which CCAT2 promotes CRC. LncRNAs act as miRNA/mRNA sponges.

The association of lncRNA CCAT2 with miRNA in CRC remains to be elucidated. Nonetheless, our study here showed that CCAT2/TAF15/RAB14/AKT/GSK3 β can serve as potential diagnostic and prognostic biomarkers for the treatment of CRC.

MATERIALS AND METHODS

Clinical Samples

A total of 44 paired samples of human CRC and adjacent normal tissues were collected at Shengjing hospital, China Medical University, China. Human colorectal cancer (CRC) tissue and matched adjacent normal tissue from the same patient were collected with the patient consent at the time of operation. The research was approved by the Ethics Committee of Shengjing hospital, China Medical University, China, and was performed in accordance with the Declaration of Helsinki.

RNA Extraction and Real-Time Quantitative PCR (qPCR)

Total RNAs were isolated from tissues or cells with Trizol reagent (Invitrogen, Shanghai). Five μ g of RNA were reverse-transcribed into cDNA using M-MLV reverse transcriptase (Promega, USA). A cDNA template was used to amplify CCAT2. qPCR was carried

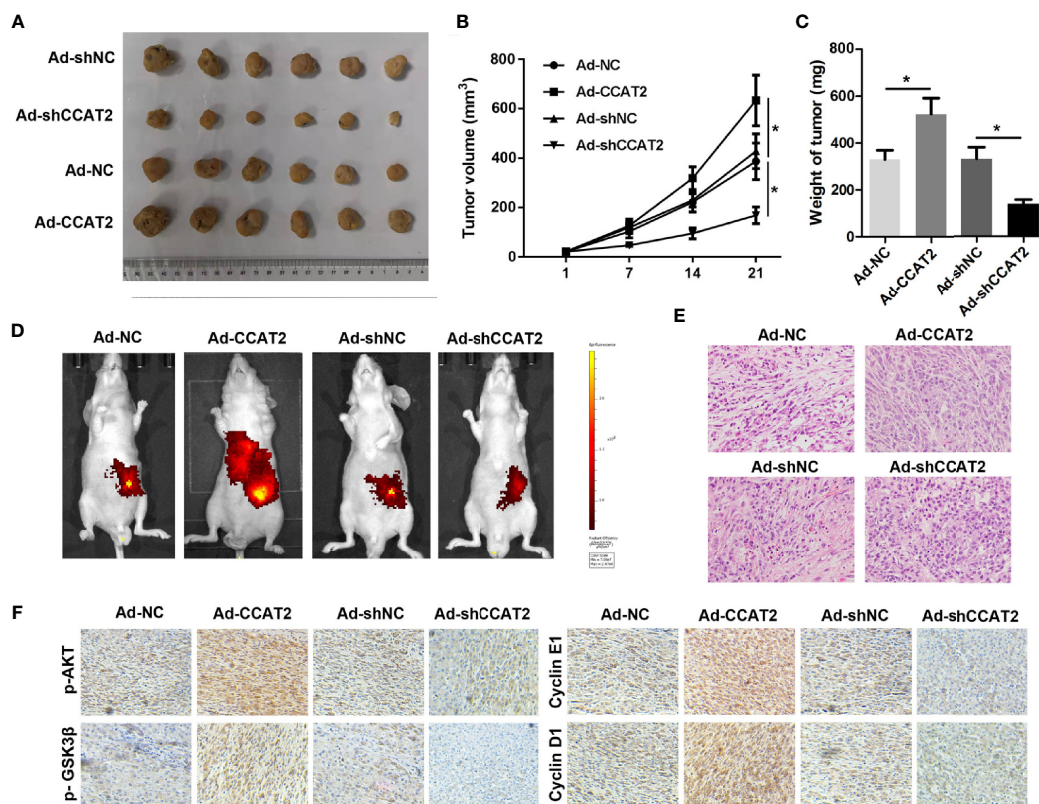


FIGURE 8 | CCAT2 promoted the subcutaneous xenograft growth of colorectal cancer cells and hepatic metastasis in nude mice. **(A)** SW620 cells infected with Ad-CCAT2, Ad-shCCAT2 or their controls were subcutaneously injected into the back of nude mice. The tumors that developed were resected and visualized. **(B)** The growth curve of the tumors in each group was analyzed. **(C)** Average tumor volume and weight indicated that CCAT2 inhibited tumor growth *in vivo*. **(D)** Bioluminescent imaging was used to detect SW620 metastasis. **(E)** HE staining was performed to evaluate the EMT potential of SW620 cells in each group ($\times 200$). The data are represented as mean \pm SD. Three independent biological repeats were used for each analysis. * $P < 0.05$ **(F)** IHC was performed to evaluate the expression of p-AKT, p-GSK3 α , cyclin D1 and cyclin E1.

out using a SYBR Premix Ex Taq kit (TaKaRa, Dalian) in a FAST7500 real-time PCR system (ABI, USA). The specific primer pairs were as follows: CCAT2 forward: 5'CTTCCAGCTCCACCTCTGAC3', reverse: 5'GAGCTCAAAGGACGATGAGG3'; RAB14 forward: 5'GACAGATGCAAGGAATCTCACC3', reverse: 5'GCTTCGAGGAACAATAAGCCAT3' β -actin forward: 5'AGTGTGACGTGGACATCCGCAAAG3', 5'ATCCACATCTGCTGGAAGGTGGAC3'.

Cell Culture and Transfection

Human CRC cell lines SW620, SW480, HT-29, LOVO, HCT116, DLD-1 and M5 and the normal colorectal epithelial HFC cell line were purchased from the Chinese Academy of Sciences, China. All cell lines were cultured in DMEM medium (Gibco, USA), and supplemented with 10% fetal bovine serum (FBS), 100 IU/ml penicillin, and 100 μ g/ml streptomycin. Cells were incubated at 37°C in a humidified chamber supplemented with 5% CO₂. The adenovirus overexpressing or silencing CCAT2 and their negative controls were established by Genepharma (Shanghai, China). Cells were infected with the adenovirus at a multiplicity of infection (MOI) of 200.

CCK-8 Assay

After infection for 12 h, SW620 and LOVO cells in each group were seeded onto a 96-well plate and then cultured at 37°C, and 5% CO₂ for 48 h. Thereafter, CCK-8 assay was carried out at 0, 24, 48 and 72 h. At each time point, 10 μ l CCK-8 was added to each well after the medium was replaced. Following incubation for another 4 h at 37°C, absorbance was measured at 450 nm in a microplate reader (Biorad, USA).

Colony Formation Assay

Following infection for 12 h, the SW620 and LOVO (200 cells per well) cells were transferred to 12-well plates with DMEM medium supplemented with 10% FBS. The cells were cultured at 37°C and 5% CO₂ for two weeks. Subsequently, the cell colonies were fixed with 4% paraformaldehyde and stained with 0.1% crystal violet (Beyotime, Shanghai, China) for 20 min at room temperature, and the colonies were counted.

EdU Staining

SW620 and LOVO cells (1.5 \times 10⁵ cells/well) were cultured in 24-well plates and infected with Ad-CCAT2, Ad-shCCAT2 or control

adenovirus for 24 h. Afterwards, 50 μ M EdU (Yuheng, Suzhou, China) was added to these cells and incubated for another 2 h. Afterward, cells were washed thrice with PBS and fixed with 4% paraformaldehyde, followed by staining with Apollo staining solution and DAPI. Finally, cell proliferation was assessed by counting cells using a light microscope (Nikon, Japan).

Transwell Cell Migration Assay

12 h after of infection, SW620 and LOVO cells were suspended in serum-free DMEM medium. Cells at a density of 3×10^5 cells/ml were seeded onto the top chamber of Transwell 24-well plates (Corning, USA). Then, 600 μ l DMEM medium containing 15% FBS was added into the lower chamber. After being cultured at 37°C for 24 h, the cells under the surface of the lower chamber were fixed with 4% paraformaldehyde followed by staining with crystal violet (0.1%, Beyotime, Shanghai, China) at room temperature for 30 min. Cell migration was evaluated by counting the cells that had migrated into the filters using an optical microscope (Nikon, Japan).

Transwell Cell Invasion Assay

In the invasion assay, 50 μ l BD Matrigel™ (BD, USA) was added on to the transwell upper chamber and placed in a 37°C incubator for 2 h to solidify. The following experiment was performed similarly as above mentioned in the migration assay.

Wound Healing Assay

Wound-healing assay was used to measure cell migration capacity in response to CCAT2 treatment. SW620 and LOVO cells were seeded in 6-well plates after infection until the confluence reached 90%. The cell monolayers were scratched with a micropipette tip to make a gap. The cell culture surface was washed three times with PBS to remove cellular debris and incubated in DMEM medium containing 2% FBS. Images were taken with an optical microscope (Nikon, Japan) 48 h later and the distance between two lines was measured and quantitated.

RNA Immunoprecipitation (RIP) and RNA Pull Down Assay

RIP and RNA pull-down assay were carried out using EZ-Magna RIP RNA-Binding Protein Immunoprecipitation Kit (Millipore, USA) and Pierce Magnetic RNA-Protein Pull-Down Kit (Thermo, USA), respectively, according to the manufacturers' instructions. The CCAT2 probe labeled with biotin was commercially purchased from GenePharma (Shanghai, China) and then incubated with streptavidin magnetic beads (Invitrogen, USA) for 1.5 h at 37°C, followed by incubation with the lysates from SW620 and LOVO cells at 4°C overnight. Finally, total extracts of SW620 and LOVO cells were prepared and was subjected to silver staining and Western blotting.

Western Blot Analysis

Protein samples from cells were extracted by RIPA buffer (Beyotime, China) and separated in 10% SDS-PAGE gels and then transferred to PVDF membranes (Millipore, USA). The membranes were incubated with primary antibodies (anti-p-AKT-phosphoT308, 1:1000, abcam, England; anti-AKT, 1:1000, abcam, England; anti-

p-GSK3 β -phosphoS9, 1:1000, abcam, England; anti-GSK3 β , 1:1000, abcam, England; cyclinD1, 1:500, Proteintech, China; cyclinE1, 1:500, Proteintech, China; p21, 1:1000, Proteintech, China; β -catenin, 1:500, Proteintech, China; vimentin, 1:500, Proteintech, China; E-cadherin, 1:500, Proteintech, China; N-cadherin, 1:500, Proteintech, China; TAF15, 1:500, Proteintech, China; RAB14, 1:500, abcam, England) overnight and then incubated with the corresponding secondary antibody. Band intensity was measured using chemiluminescence (ECL) system kit according to the manufacturer's instructions (Solarbio, Beijing, China). The optical densities (OD) value was analyzed with ImageJ software (NIH, Bethesda, MD, USA).

FISH Assay

For Fluorescence *in situ* hybridization (FISH) assay, 48 h after adenovirus infection, cells were fixed with 4% paraformaldehyde for 20 min, permeabilized with 0.05% triton for 5 min, and then blocked with 10% donkey serum for 1 h. After fixation, cells were incubated with CCAT2 probe (GenePharma, China) for 1 h. The nuclei were stained with DAPI for 5 min, and the optical microscope (Nikon, Japan) was used for observation. The sequence of the probe is Biotin-TTTTCCATTTGTGCGAG AGAGCGGGTGTCTCTGAGGACCGCACAG.

Dual Luciferase Reporter Assay

Based on bioinformatics predictions, we found that RAB14 was regulated by TAF15. The promoter segments of RAB14 were obtained by PCR and inserted into pGL4.10 vector. 250 ng reporter vector, 250 ng overexpressing vector or siRNA, and 10 ng pRL-SV40 vector were transfected with Lipofectamine 3000 (Invitrogen, USA) according to the instructions. After 48 h, cells were lysed in 100 μ l of passive lysis buffer. The firefly luciferase activity and the Renilla activity were determined using a Dual-Luciferase® Reporter Assay System. For each experiment, firefly luciferase activity was normalized to Renilla activity.

Analysis of Tumor Xenografts

All the animal experiments were approved by the Ethic Committee of Shengjing hospital, China Medical University, China. For the *in vivo* growth assay, SW620 cells were injected subcutaneously into 6-week-old female BALB/C nude mice (1×10^7 cells/mice in 100 μ l of DMEM). After 7 d, sh-NC, CCAT2, shNC and shCCAT2 adenovirus were injected into the tumor body. Meanwhile, the length and width of tumors of all mice were measured every five days. Tumor volume was determined according to the equation: $V = (L \times W^2)/2$, where V is the volume, L is the length and W is the width of the tumor. On the 6th week of injection, mice were killed and tumors were harvested, weighed and imaged.

Analysis of Tumor Metastasis

We prepared SW620 cells as follows after adenovirus infection: six week old female nude mice were anaesthetized using 1% pentobarbital (40mg/kg); then, cells were transplanted intrasplenically into the mice. At the endpoint, mice were again anaesthetized using 1% pentobarbital (160mg/kg) and observed in the IVIS Spectrum living image system

(PerkinElmer, USA). The images were obtained and analyzed using ImageJ software (version 1.42q).

Hematoxylin Eosin (HE) Staining

Sliver-stained samples were separated and placed in 10% formalin overnight and embedded in paraffin. Then, the tissues were sliced into 5 μm -thick sections and fixed on a glass slide. The staining procedures were performed according to the manufacturer's instructions (Solarbio, Beijing, China). Briefly, the sections were soaked in xylene, ethanol in gradient concentration, and hematoxylin, respectively, and sealed with resin. Finally, the morphology was observed and observed under a light microscope.

Statistical Analysis

Statistical analyses were carried out using SPSS version 20.0 software and Graph Pad Prism version 6.0. The data are presented as mean \pm standard deviation (SD). A Student's *t*-test was used to evaluate the significance of the difference between two groups. $P < 0.05$ was considered to represent a statistically-significant difference.

REFERENCES

- Siegel RL, Miller KD, Fedewa SA, Ahnen DJ, Meester RGS, Barzi A, et al. Colorectal Cancer Statistics, 2017. *CA Cancer J Clin* (2017) 67(3):177–93. doi: 10.3322/caac.21395
- Weinberg BA, Marshall JL, Salem ME. The Growing Challenge of Young Adults With Colorectal Cancer. *Oncology (Williston Park)* (2017) 31(5):381–9.
- Jemal A, Bray F, Center MM, Ferlay J, Ward E, Forman D. Global Cancer Statistics. *CA Cancer J Clin* (2011) 61(2):69–90. doi: 10.3322/caac.20107
- Moriarty A, O'Sullivan J, Kennedy P, Mehigan B, McCormick P. Current Targeted Therapies in the Treatment of Advanced Colorectal Cancer: A Review. *Ther Adv Med Oncol* (2016) 8(4):276–93. doi: 10.1177/1758834016646734
- Zhai Z, Yu X, Yang B, Zhang Y, Zhang L, Li X, et al. Colorectal Cancer Heterogeneity and Targeted Therapy: Clinical Implications, Challenges and Solutions for Treatment Resistance. *Semin Cell Dev Biol* (2017) 64:107–15. doi: 10.1016/j.semcdb.2016.08.033
- Huarte M. The Emerging Role of lncRNAs in Cancer. *Nat Med* (2015) 21(11):1253–61. doi: 10.1038/nm.3981
- Sun M, Nie F, Wang Y, Zhang Z, Hou J, He D, et al. lncRNA HOXA11-AS Promotes Proliferation and Invasion of Gastric Cancer by Scaffolding the Chromatin Modification Factors PRC2, LSD1, and DNMT1. *Cancer Res* (2016) 76(21):6299–310. doi: 10.1158/0008-5472.CAN-16-0356
- Sun M, Nie FQ, Wang ZX, De W. Involvement of lncRNA Dysregulation in Gastric Cancer. *Histol Histopathol* (2016) 31(1):33–9. doi: 10.14670/HH-11-655
- Wang CJ, Zhu CC, Xu J, Wang M, Zhao WY, Liu Q, et al. The lncRNA UCA1 Promotes Proliferation, Migration, Immune Escape and Inhibits Apoptosis in Gastric Cancer by Sponging Anti-Tumor miRNAs. *Mol Cancer* (2019) 18(1):115. doi: 10.1186/s12943-019-1032-0
- Wang F, Zhu W, Yang R, Xie W, Wang D. lncRNA ZEB2-AS1 Contributes to the Tumorigenesis of Gastric Cancer via Activating the Wnt/beta-Catenin Pathway. *Mol Cell Biochem* (2019) 456(1-2):73–83. doi: 10.1007/s11010-018-03491-7
- Wang X, Kan J, Han J, Zhang W, Bai L, Wu H. lncRNA SNHG16 Functions as an Oncogene by Sponging MiR-135a and Promotes JAK2/STAT3 Signal Pathway in Gastric Cancer. *J Cancer* (2019) 10(4):1013–22. doi: 10.7150/jca.29527
- Han P, Li JW, Zhang BM, Lv JC, Li YM, Gu XY, et al. The lncRNA CRNDE Promotes Colorectal Cancer Cell Proliferation and Chemoresistance via miR-181a-5p-Mediated Regulation of Wnt/beta-Catenin Signaling. *Mol Cancer* (2017) 16(1):9. doi: 10.1186/s12943-017-0583-1
- Wu K, Jiang Y, Zhou W, Zhang B, Li Y, Xie F, et al. Long Noncoding RNA RC3H2 Facilitates Cell Proliferation and Invasion by Targeting MicroRNA-

DATA AVAILABILITY STATEMENT

The original contributions presented in the study are included in the article/supplementary material. Further inquiries can be directed to the corresponding author.

ETHICS STATEMENT

Written informed consent was obtained from the individual(s) for the publication of any potentially identifiable images or data included in this article.

AUTHOR CONTRIBUTIONS

DW and ZL did the experiments and analyzed the data. HY supervised the research. All authors contributed to the article and approved the submitted version.

- 101-3p/EZH2 Axis in OSCC. *Mol Ther Nucleic Acids* (2020) 20:97–110. doi: 10.1016/j.omtn.2020.02.006
14. Cao W, Liu JN, Liu Z, Wang X, Han ZG, Ji T, et al. A three-lncRNA Signature Derived From the Atlas of ncRNA in Cancer (TANRIC) Database Predicts the Survival of Patients With Head and Neck Squamous Cell Carcinoma. *Oral Oncol* (2017) 65:94–101. doi: 10.1016/j.oraloncology.2016.12.017
15. Liu J, Xing Y, Xu L, Chen W, Cao W, Zhang C. Decreased Expression of Pseudogene PTENP1 Promotes Malignant Behaviours and Is Associated With the Poor Survival of Patients With HNSCC. *Sci Rep* (2017) 7:41179. doi: 10.1038/srep41179
16. Liu Z, Zhou W, Lin C, Wang X, Zhang X, Zhang Y, et al. Dysregulation of FOXD2-AS1 Promotes Cell Proliferation and Migration and Predicts Poor Prognosis in Oral Squamous Cell Carcinoma: A Study Based on TCGA Data. *Aging (Albany NY)* (2020) 13(2):2379–96. doi: 10.18632/aging.202268
17. Hu J, Shan Y, Ma J, Pan Y, Zhou H, Jiang L, et al. lncRNA ST3Gal6-AS1/ST3Gal6 Axis Mediates Colorectal Cancer Progression by Regulating Alpha-2,3 Sialylation via PI3K/Akt Signaling. *Int J Cancer* (2019) 145(2):450–60. doi: 10.1002/ijc.32103
18. Lin H, Guo Q, Lu S, Chen J, Li X, Gong M, et al. lncRNA SUMO1P3 Promotes Proliferation and Inhibits Apoptosis in Colorectal Cancer by Epigenetically Silencing CPEB3. *Biochem Biophys Res Commun* (2019) 511(2):239–45. doi: 10.1016/j.bbrc.2019.02.006
19. Lv SY, Shan TD, Pan XT, Tian ZB, Liu XS, Liu FG, et al. The lncRNA ZEB1-AS1 Sponges miR-181a-5p to Promote Colorectal Cancer Cell Proliferation by Regulating Wnt/beta-Catenin Signaling. *Cell Cycle* (2018) 17(10):1245–54. doi: 10.1080/15384101.2018.1471317
20. Wang J, Tian Y, Zheng H, Ding Y, Wang X. An Integrated Analysis Reveals the Oncogenic Function of lncRNA LINC00511 in Human Ovarian Cancer. *Cancer Med* (2019) 8(6):3026–35. doi: 10.1002/cam4.2171
21. Yao N, Yu L, Zhu B, Gan HY, Guo BQ. lncRNA GIHCG Promotes Development of Ovarian Cancer by Regulating microRNA-429. *Eur Rev Med Pharmacol Sci* (2018) 22(23):8127–34. doi: 10.26355/eurrev_201812_16504
22. Zeng XY, Jiang XY, Yong JH, Xie H, Yuan J, Zeng D, et al. lncRNA ABHD11-AS1, Regulated by the EGFR Pathway, Contributes to the Ovarian Cancer Tumorigenesis by Epigenetically Suppressing TIMP2. *Cancer Med* (2019) 8(16):7074–85. doi: 10.1002/cam4.2586
23. Kong FR, Lv YH, Yao HM, Zhang HY, Zhou Y, Liu SE. lncRNA PCAT6 Promotes Occurrence and Development of Ovarian Cancer by Inhibiting PTEN. *Eur Rev Med Pharmacol Sci* (2019) 23(19):8230–8. doi: 10.26355/eurrev_201910_19132
24. Ling H, Spizzo R, Atlasi Y, Nicoloso M, Shimizu M, Redis RS, et al. CCAT2, a Novel Noncoding RNA Mapping to 8q24, Underlies Metastatic Progression

- and Chromosomal Instability in Colon Cancer. *Genome Res* (2013) 23 (9):1446–61. doi: 10.1101/gr.152942.112
25. Tian FM, Meng FQ, Wang XB. Overexpression of Long-Noncoding RNA ZFAS1 Decreases Survival in Human NSCLC Patients. *Eur Rev Med Pharmacol Sci* (2016) 20(24):5126–31.
 26. Bai J, Xu J, Zhao J, Zhang R. lncRNA SNHG1 Cooperated With miR-497/miR-195-5p to Modify Epithelial-Mesenchymal Transition Underlying Colorectal Cancer Exacerbation. *J Cell Physiol* (2019) 235(2):1453–68. doi: 10.1002/jcp.29065
 27. Bai JG, Tang RF, Shang JF, Qi S, Yu GD, Sun C. Upregulation of Long Noncoding RNA CCAT2 Indicates a Poor Prognosis and Promotes Proliferation and Metastasis in Intrahepatic Cholangiocarcinoma. *Mol Med Rep* (2018) 17(4):5328–35. doi: 10.3892/mmr.2018.8518
 28. Cai H, Ye X, He B, Li Q, Li Y, Gao Y. lncRNA-AP001631.9 Promotes Cell Migration in Gastric Cancer. *Int J Clin Exp Pathol* (2015) 8(6):6235–44.
 29. Guo H, Hu G, Yang Q, Zhang P, Kuang W, Zhu X, et al. Knockdown of Long Non-Coding RNA CCAT2 Suppressed Proliferation and Migration of Glioma Cells. *Oncotarget* (2016) 7(49):81806–14. doi: 10.18632/oncotarget.13242
 30. Hosseini ES, Meryet-Figuere M, Sabzalipoor H, Kashani HH, Nikzad H, Asemi Z. Dysregulated Expression of Long Noncoding RNAs in Gynecologic Cancers. *Mol Cancer* (2017) 16(1):107. doi: 10.1186/s12943-017-0671-2
 31. Huang S, Qing X, Huang Z, Zhu Y. The Long Non-Coding RNA CCAT2 Is Up-Regulated in Ovarian Cancer and Associated With Poor Prognosis. *Diagn Pathol* (2016) 11(1):49. doi: 10.1186/s13000-016-0499-x
 32. Qiu M, Xu Y, Yang X, Wang J, Hu L, Xu L, et al. CCAT2 Is a Lung Adenocarcinoma-Specific Long Non-Coding RNA and Promotes Invasion of Non-Small Cell Lung Cancer. *Tumour Biol* (2014) 35(6):5375–80. doi: 10.1007/s13277-014-1700-z
 33. Siddique H, Al-Ghafari A, Choudhry H, Alturki S, Alshaibi H, Al Doghathier H, et al. Long Noncoding RNAs as Prognostic Markers for Colorectal Cancer in Saudi Patients. *Genet Test Mol Biomarkers* (2019) 23(8):509–14. doi: 10.1089/gtmb.2018.0308
 34. Fosselteder J, Calin GA, Pichler M. Long Non-Coding RNA CCAT2 as a Therapeutic Target in Colorectal Cancer. *Expert Opin Ther Targets* (2018) 22 (12):973–6. doi: 10.1080/14728222.2018.1541453
 35. Ozawa T, Matsuyama T, Toiyama Y, Takahashi N, Ishikawa T, Uetake H, et al. CCAT1 and CCAT2 Long Noncoding RNAs, Located Within the 8q.24.21 'Gene Desert', Serve as Important Prognostic Biomarkers in Colorectal Cancer. *Ann Oncol* (2017) 28(8):1882–8. doi: 10.1093/annonc/mdx248
 36. Pan L, Li Y, Jin L, Li J, Xu A. TRPM2-AS Promotes Cancer Cell Proliferation Through Control of TAF15. *Int J Biochem Cell Biol* (2020) 120:105683. doi: 10.1016/j.biocel.2019.105683
 37. Chen TW, Yin FF, Yuan YM, Guan DX, Zhang E, Zhang FK, et al. CHML Promotes Liver Cancer Metastasis by Facilitating Rab14 Recycle. *Nat Commun* (2019) 10(1):2510. doi: 10.1038/s41467-019-10364-0
 38. Yang S, Zhang X, Qu H, Qu B, Yin X, Zhao H. Cabozantinib Induces PUMA-Dependent Apoptosis in Colon Cancer Cells via AKT/GSK-3beta/NF-kappaB Signaling Pathway. *Cancer Gene Ther* (2019) 27(5):368–77. doi: 10.1038/s41417-019-0098-6
 39. Yu W, Liu C, Li X, Yang F, Cheng L, Liu C, et al. Inositol Hexaphosphate Suppresses Colorectal Cancer Cell Proliferation via the Akt/GSK-3beta/Beta-Catenin Signaling Cascade in a 1,2-Dimethylhydrazine-Induced Rat Model. *Eur J Pharmacol* (2017) 805:67–74. doi: 10.1016/j.ejphar.2017.03.011
 40. Yuan G, Zhang B, Yang S, Jin L, Datta A, Bae S, et al. Novel Role of STRAP in Progression and Metastasis of Colorectal Cancer Through Wnt/beta-Catenin Signaling. *Oncotarget* (2016) 7(13):16023–37. doi: 10.18632/oncotarget.7532
 41. Zhu Y, Zhou Q, Zhu G, Xing Y, Li S, Ren N, et al. GSK-3beta Phosphorylation-Dependent Degradation of ZNF281 by Beta-TrCP2 Suppresses Colorectal Cancer Progression. *Oncotarget* (2017) 8(51):88599–612. doi: 10.18632/oncotarget.20100
 42. Xu M, Zhang Y, Cui M, Wang X, Lin Z. Mortalin Contributes to Colorectal Cancer by Promoting Proliferation and Epithelial-Mesenchymal Transition. *IUBMB Life* (2019) 72(4):771–81. doi: 10.1002/iub.2176
 43. Xiong HG, Li H, Xiong Y, Yang QC, Yang LL, Chen L, et al. Long Noncoding RNA MYOSLID Promotes Invasion and Metastasis by Modulating the Partial Epithelial-Mesenchymal Transition Program in Head and Neck Squamous Cell Carcinoma. *J Exp Clin Cancer Res* (2019) 38(1):278. doi: 10.1186/s13046-019-1254-4
 44. Xia L, Lin J, Su J, Oyang L, Wang H, Tan S, et al. Diallyl Disulfide Inhibits Colon Cancer Metastasis by Suppressing Rac1-Mediated Epithelial-Mesenchymal Transition. *Oncotargets Ther* (2019) 12:5713–28. doi: 10.2147/OTT.S208738
 45. Xiao KH, Teng K, Ye YL, Tan L, Chen MK, Liang HT, et al. Kinesin Family Member C1 Accelerates Bladder Cancer Cell Proliferation and Induces Epithelial-Mesenchymal Transition via Akt/GSK3beta Signaling. *Cancer Sci* (2019) 110(9):2822–33. doi: 10.1111/cas.14126
 46. Wang H, Wang HS, Zhou BH, Li CL, Zhang F, Wang XF, et al. Epithelial-Mesenchymal Transition (EMT) Induced by TNF-Alpha Requires AKT/GSK-3beta-Mediated Stabilization of Snail in Colorectal Cancer. *PLoS One* (2013) 8 (2):e56664. doi: 10.1371/journal.pone.0056664

Conflict of Interest: The authors declare that the research was conducted in the absence of any commercial or financial relationships that could be construed as a potential conflict of interest.

Publisher's Note: All claims expressed in this article are solely those of the authors and do not necessarily represent those of their affiliated organizations, or those of the publisher, the editors and the reviewers. Any product that may be evaluated in this article, or claim that may be made by its manufacturer, is not guaranteed or endorsed by the publisher.

Copyright © 2021 Wang, Li and Yin. This is an open-access article distributed under the terms of the Creative Commons Attribution License (CC BY). The use, distribution or reproduction in other forums is permitted, provided the original author(s) and the copyright owner(s) are credited and that the original publication in this journal is cited, in accordance with accepted academic practice. No use, distribution or reproduction is permitted which does not comply with these terms.